$$\int_{-l/2}^{l/2}\left(\frac{\partial^2\phi_i}{\partial x^2}+\frac{\omega^2}{c^2}\phi_i\right)\phi_i^*\,dx=\frac{Z_0}{c}$$

$$\cdot\sum_n\frac{\omega^2(1\pm\cos\beta L)}{2(\omega^2-\omega_{i,n}{}^2)W_{i,n}}\int_{-l/2}^{l/2}\bar{j}_{i,n,y}\phi_i^*dx\int_{-l/2}^{l/2}\bar{j}_{i,n,y}^*\phi_i dx. \quad (66)$$

Integrating by parts the second term on the left-hand side of (66) we have

$$\frac{\omega^2}{c^2}\int_{-l/2}^{l/2}\phi_i\phi_i^*dx-\int_{-l/2}^{l/2}\frac{\partial\phi_i}{\partial x}\frac{\partial\phi_i^*}{\partial x}=\frac{Z_0}{c}$$

$$\cdot\sum_n\frac{\omega^2(1\pm\cos\beta L)}{(\omega^2-\omega_{i,n}{}^2)2W_{i,n}}\int_{-l/2}^{l/2}\bar{j}_{i,n,y}\phi_i^*dx\int_{-l/2}^{l/2}\bar{j}_i{}^*{}_{,n,y}\phi_i dx \quad (67)$$

since

$$\phi(\pm l/2)=0$$

Let us assume that $\phi_{0,i}$ and ω_0 solve (67). A trial function for the voltage is expressed as follows:

$$\phi_i(x)=\phi_{0,i}(x)+\epsilon_i(x). \quad (68)$$

Since the values of the voltage at the ends of the slot are known,

$$\epsilon_i(\pm l/2)=0. \quad (69)$$

Suppose, then, (67) yields a value of frequency ω for the trial function where

$$\omega=\omega_0+\Delta. \quad (70)$$

Then, it can be shown that Δ is of the second order in ϵ_i. Thus (67) is a variational form of the solution.

ACKNOWLEDGMENT

The authors are indebted to Prof. M. Chodorow for many helpful discussions.

Microphony in Waveguide*

I. GOLDSTEIN† AND S. SOORSOORIAN†

Summary—**This paper describes the mechanism of phase modulation by waveguide in the presence of a high intensity acoustic field. X-band rectangular was studied to determine the following:**

a) Resonant frequency in a transverse vibrational mode.

b) Means of minimizing phase modulation.

A CW radar can be represented as a microwave bridge in which the transmitted signal is compared in frequency with the received signal so that Doppler information may be obtained. Any disturbance of the bridge at the Doppler frequency will cause degradation in system sensitivity. It is our purpose to show that waveguide under a high acoustical field can definitely contribute to microphonics via the mechanism of phase modulation. This can be accomplished in many ways to a waveguide but we are primarily interested in transverse motion. The different transverse modes for the top and side waveguide walls are shown in Fig. 1.

Phase shift is accomplished by the motion of the side walls. The incremental phase shift is expressed as the following relationship for a rectangular waveguide operating in the TE_{10} mode:

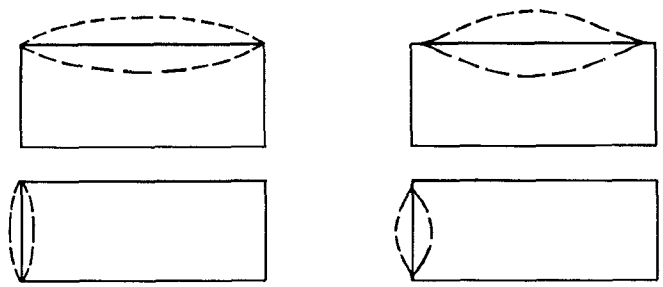

Fig. 1—First-mode vibration shapes.

$$d\phi=\frac{\pi l\lambda_g da}{2a^3},$$

$d\phi$ = incremental change of phase,
da = incremental change of side wall,
a = wide dimension of the waveguide,
l = length of the waveguide,
λ_g = guide wavelength.

Fig. 1 indicates an ideal situation of no coupling between waveguide walls. However, in actual practice there is coupling between the motion of the wide walls

* Manuscript received by the PGMTT, November 19, 1959; revised manuscript received, January 21, 1960.

† Raytheon Company, Bedford, Mass.

and narrow sides of the waveguide, as will be shown in the section on experimental results.

For the sake of analysis, the sides of the waveguide can be represented as simple beams. The resonant frequencies for the bending vibration of simple beams can be expressed in one simple form,

$$f = \frac{bc_1 t}{d^2}, \qquad (1)^1$$

where

f = frequency in cycles per second,
b = a constant dependent on shape and mode,
c_1 = the longitudinal wave velocity for the material,
t = the thickness,
d = a characteristic length.

A definition of the pin-pin and clamp-clamp boundary condition is in order. As shown in Fig. 1, the pin-pin condition is one in which there is a definite slope of the beam deflection at the boundaries. The clamp-clamp condition is one in which there is zero slope of the beam deflection at the boundaries.

In (1) for the resonant frequencies,

$b = 0.45$ for pin-pin condition,
$b = 1.01$ for the clamp-clamp condition.

Fig. 2 shows the typical acoustical environment for a large missile and the simulated conditions. Various samples of waveguide were made part of a microwave bridge and excited by a tweeter placed one inch from the broad face. Fig. 3 shows a schematic of the complete system. Power from a frequency stabilized microwave source was fed into the microwave circuit. One arm acts as the local oscillator when modulated by a 30-mc oscillator. A sideband is extracted through a tunable high Q cavity and is observed on a microwave spectrum analyzer. The other arm containing the RF carrier enters a microwave bridge where the carrier is suppressed by an adjustable phase shifter. Acoustical energy exciting the test piece at resonant frequencies will cause the bridge to unbalance because of the dimensional changes in the test piece; the side bands resulting from this phase modulation mix with the local oscillator to provide a phase-modulated 30-mc output for the IF amplifiers. It is then balance-bridge detected and fed into a video amplifier through a band-pass filter, and a visual display shows the relative amplitudes and resonant frequencies.

To calibrate the station, a ferrite modulator is substituted for the piece under test and driven at various side frequencies and levels to obtain a calibration curve. The following relationship yields the power in the sidebands:

$$P_{sB} = \frac{(\theta_{max})^2}{16}^2,$$

where θ = phase shift in the test arm.

[1] P. M. Morse, "Vibration and Sound," McGraw-Hill Book Co., Inc., New York, N. Y., 2nd ed.; 1948.
[2] Derived in the Appendix.

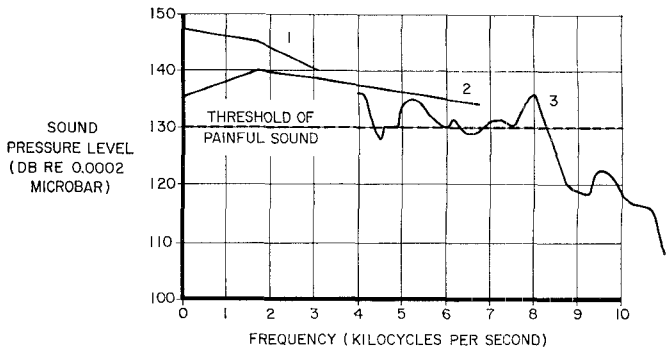

Fig. 2—Near-field spectrum of rocket noise. Curve 1, solid propellant with re-ignition of exhaust gases downstream of exit. Curve 2, solid propellant that does not re-ignite. Curve 3, sound level of test station.

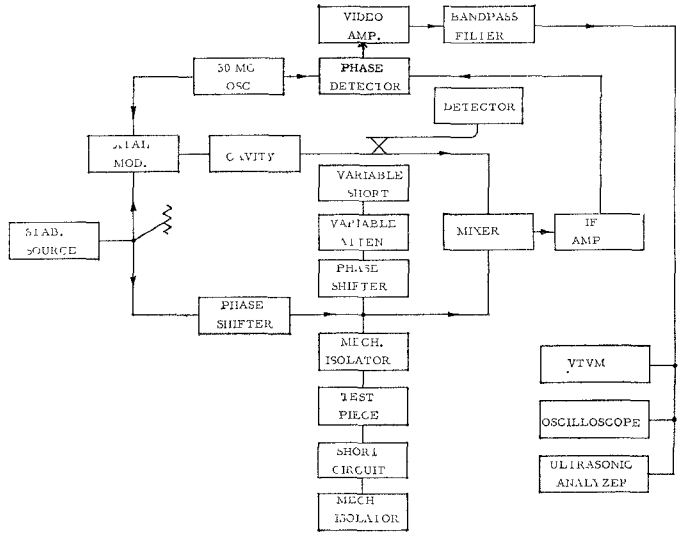

Fig. 3—Microphonic test station.

Incidentally, the sensitivity of the system is greater than 0.003 degree of phase shift.

Two areas were studied,

a) various waveguide geometries,
b) effectiveness of various coating materials on the outside of the waveguide to act as acoustical and vibrational dumping agents.

Fig. 4 shows the geometries of an X-band waveguide tested along with a simulation of the pin-pin and clamp-clamp conditions. Incidentally, the resonant frequencies of the narrow sides (0.4×0.9 ID), which are 28.4 kc pinned and 64.6 kc clamped, were not observed. Essentially then, phase modulation was caused by the motion of the wide walls (top and bottom) at their resonant frequencies coupling to the side walls. Fig. 5 shows a table of results. Note that for waveguide thicknesses greater than 0.2 inch no output was observed. Fig. 6 shows results which indicate that to a first order at least, the resonant frequencies of different waveguides were independent of length. The conclusion drawn is that truly transverse resonant effects have been observed.

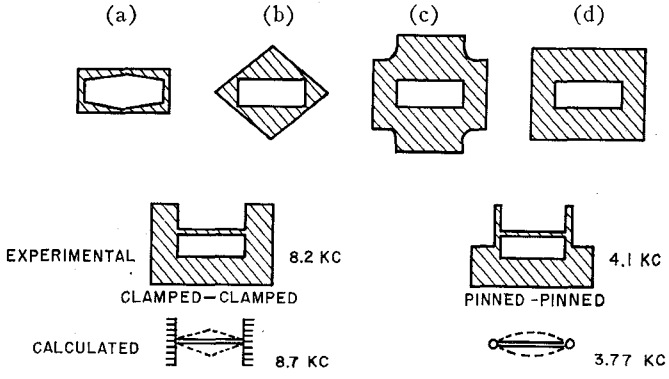

Fig. 4—Waveguide geometries.

Configuration	Wall Thickness	Measured Resonant Frequency kc	Relative Amplitude, Volts
Tapered (a)	—	6.0	0.5
Diamond (b)	—	3.5	0.5
Cross (c)	—	—	—
Heavy Wall (d)	0.300	—	—
Heavy Wall	0.200	—	—
Heavy Wall	0.150	11.7	0.015
Heavy Wall	0.125	10.2	0.075
Heavy Wall	0.100	8.4	0.40
Heavy Wall	0.075	7.3	1.50
Conventional	0.050	5.9	20+*
Light Wall	0.025	3.2	20+*

* Saturation noise level≅0.015 volt, $f=bc_1t/d^2$.

Fig. 5—Resonant frequencies and relative amplitude for various waveguide configurations. Material: brass; length 12 inches; 0.400×0.900 ID.

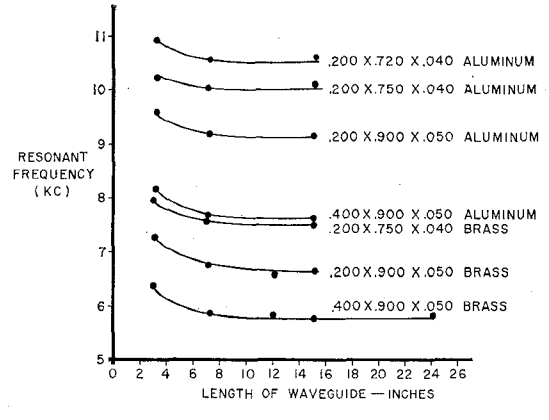

Fig. 6—Waveguide natural resonant frequencies.

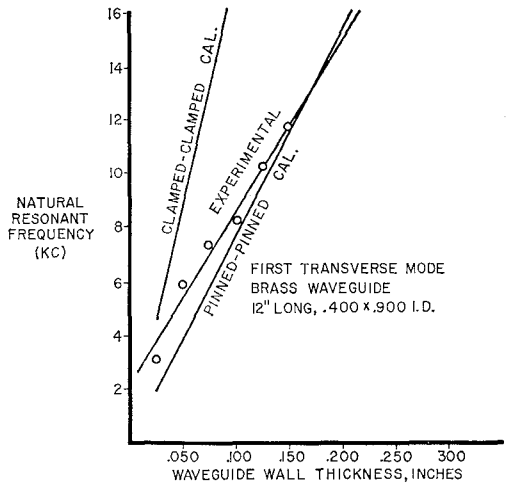

Fig. 7.

Thickness	Frequency Pin	Frequency Clamp	$\frac{f_{pin}+f_{clamp}}{2}$	$f_{Exp.}$
Inch	KC Calculated	KC Calculated	KC Calculated	
0.150	11.20	25.70	18.40	11.7
0.125	9.41	21.20	15.30	10.2
0.100	7.55	17.40	12.47	8.4
0.075	5.70	13.10	9.40	7.3
0.050	3.77	8.70	6.23	5.9
0.025	1.87	4.16	2.98	3.2

Fig. 8.

Description of Coating Materials	Resonant Frequency KC	Relative Amplitude, Volts	−DB from Uncoated Guide
Aquaplas F50/180A	7.6	0.13	43.6
Aquaplas F102A	6.4	0.20	40.0
Johns-Manville No. 678	5.3	0.33	35.6
Minnesota Mining & Mfg. EC-822	5.7	3.50	34.0
Johns-Manville No. 806	5.5	0.60	30.4
Aquaplas F100A	6.9	0.60	30.4
Minnesota Mining & Mfg. EC-244	5.6	0.90	27.0
Minnesota Mining & Mfg. EC-549	5.6	1.00	26.08
Tesamoll $\frac{1}{4}''$	5.8	3.50	15.2
Johns-Manville No. V20	5.7	5.0	12.0
Tesamoll $\frac{1}{8}''$	5.8	8.00	8.0
Stabond C-890	5.7	8.80	7.2
Johns-Manville D.B. C.T.	5.8	15.0	2.6
Noise Level≅0.015 Volt			

Fig. 9—Damping efficiencies of various coating materials of thickness $\frac{1}{8}$ inch. Brass waveguide 0.400×0.900 ID; 0.050 wall thickness; length 12 inches.

Fig. 7 shows the experimental and calculated results. A brief discussion is in order concerning the calculated vs the experimental values of resonant frequencies.

As shown in Fig. 8, for thinner wall waveguides the resonant frequency is approximately the average of pin-pin and clamp-clamp frequencies. With increasing thicknesses, the calculated pin-pin frequencies appear to yield a better agreement with experiment.

Fig. 9 shows a table of results using different coatings on the outside of the waveguide. Unfortunately the coating which appeared to be the best suffered from the following characteristics:

a) variation in acoustic attenuation with temperature,
b) solubility in water.

This area is a promising one and more research is needed in acoustic damping materials. This bridge technique has been used as a general tool for detecting resonances in microwave components and particularly high power microwave tubes. Mention should be made of a technique that can be used in most laboratories, that of an air blast. An air hose using a $\frac{1}{4}$-inch nozzle and 40 pounds of air pressure has been used and found sufficient to excite resonances up to 50 kc.

Conclusion

It has been shown that a high acoustic field can produce phase modulation of a waveguide, which can seriously degrade any system where Doppler information is desired. Methods of minimizing this effect have been demonstrated.

There is still a need for getting the best microwave structures for components such as magic "T's," hybrids, mixers, directional couplers, etc., which have minimum phase variation in an acoustical field.

Appendix

If we let the input voltage to the bridge be $V_{in} = E_n \sin \omega t$ in the null arm, we have

$$e = \frac{E_n}{2} \sin \omega t \sin \theta,$$

where

$$\theta = \text{phase shift in test arm} = k \sin \omega_p t,$$

$$e = \frac{E_n}{2} \sin \omega t \sin (k \sin \omega_p t)$$

$$= \frac{E_n}{2} \sin \omega t \left[2 \sum_{n=0} J_{(2n+1)}(k) \sin (2x + 1)\omega_p t \right].$$

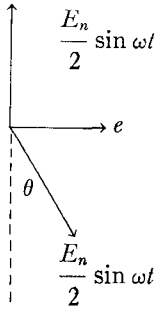

With expansion and modification of this last equation, the following results:

$$\frac{\text{First sideband power}}{\text{Incident power}} = P_{sB} = \frac{[J_1(k)]^2}{4}.$$

For small values of k, J_1, $(k) \approx K/2 \approx \theta$,

$$\therefore \; P_{sB} = \frac{(\theta_{\max})^2}{16}.$$